arXiv:1404.7805v1 [cond-mat.mtrl-sci] 30 Apr 2014

# Equations of state of magnesium perovskite and postperovskite: diagnostics from ab initio simulations

Roman Belousov Mauro Prencipe

May 1, 2014

**Abstract**

The isothermal compression of magnesium perovskite and postperovskite is examined through the F-f plot and the diagnostic plot of Vinet universal model theoretically from the ab initio quantum-mechanical calculations at the hybrid Hartree-Fock / Density Functional Theory level. A purely numerical approach, first time applied in this paper, shows that the discrepancies largely observed between studies on the perovskite and criticized in geophysical applications are due to the inadequate choice of the Birch-Murnaghan equation of state; meanwhile the Vinet model is found utterly appropriate for the mineral and infers consistent estimations of the bulk modulus and its pressure derivative. The diagnostics of the postperovskite suggest similar conclusions.

## 1 Introduction

The family of magnesium perovskite (Mg,Fe)$SiO_3$ (space group *Pbnm*) is widely considered as the most abundant constituent of the lower Earth mantle ( 75 Vol. % Ref. [23]). It was thoroughly studied with various ever improving techniques due to its importance in geophysics. The existence of post-perovskite polymorphic structure (space group *Cmcm*), recently discovered and described in Ref. [22, 21]), provided for the mineralogical reasons of geophysical anomalies met in the $D''$-layer (mantle-core boundary), exciting interest in precise thermodynamic properties of the phases.

In this paper the $MgSiO_3$ members of minral families are studied. To infer the isothermal bulk moduli and their pressure/temperature dependence, which are essential for the interpretation of seismological data, many efforts were devoted to establish the isothermal Equation of States (EoS) for each mineral by theoretical and experimental means. However 2 problems, that did not reach a satisfactory state of understanding, can be traced through the existing publications.

At first, as noted in Ref. [28], the thermodynamics asserts that the adiabatic bulk modulus must be greater than the isothermal bulk modulus, whereas systematically upon the comparison of measurements on the magnesium perovskite one finds the contrary relation between them, which is hardly explained by the precision. Indeed, the values of isothermal bulk moduli as reported by many X-ray compression experiments usually agree quite well, e.g. Ref. [36, 11, 14, 28, 17, 6, 29, 7, 33]. Compared to the adiabatic bulk moduli, they differ notably from the results of Brillouin spectroscopy and shock-wave loading techniques (Ref. [37, 30, 3, 16, 20]), that as direct measurements are expected to have a superior accuracy. The discrepancy, once attributed to the experimental errors, requires to accept a large uncertainty which is unsatisfactory for geophysical applications Ref. [33, 3]. Moreover, the values of bulk modulus pressure derivative stand out of the range commonly found for solids.

The second issue becomes evident when considering the theoretical works, e.g. Ref. [10, 19, 18, 32, 23], which claim generally to reproduce the experimental results. Indeed, numerically the predicted properties are found in a remarkable agreement for the accuracy in this class of works. Nonetheless, the major part of theoretical publications prefer the (Rose-)Vinet model of compression (VEoS), like in Ref. [19, 18, 32, 23], to the Birch-Murnaghan EoS (BMEoS), which is almost ubiquitously adopted in the experiments. In fact, BMEoS (Ref. [10]) appears to perform worse on numerical comparison.

In fact, the choice of EoS can be justified by means of the designed diagnostics on the compression data, such as the F-f plots for BMEoS or the analogous technique for VEoS (Ref. [2]). Strictly speaking, the diagnostics should be applied, as usually done, to reassure that the prerequisite assumptions implied by the suggested EoS are satisfied Ref. [31]. Though the most of publications do not discuss it, a review of the so called F-f plots on different data sources is available in Ref. [20], which argues for large discrepancies between the analyzed results.

The perovskite and postperovskite are delicate subjects for isothermal compression experiments. For these minerals are high-pressure phases, they are very stiff and undergo very small changes of volume measured by the X-ray diffraction techniques in response to pressure. Consequently, the experiment requires very precise and accurate measurements and pressure loading of extremely wide range which are both difficult to carry out. The technical challenge is naturally accompanied by larger errors. They contribute strongly to the observed uncertainties. Meanwhile the theoretical data do not suffer precision losses due to the stiffness of material or ranges of pressure.

With the present work we intend to show by using theoretical ab-initio quantum-mechanical calculations that both issues are likely to stem from the same source. An advanced mathematical approach, that we devise, is applied first time for the theoretical diagnostics of EoS. It reveals that BMEoS of lower orders, as adopted regularly in the isothermal X-ray compression studies, is inadequate model for the magnesium perovskite: the inferred parameters overestimate the isothermal bulk modulus and undervalue the pressure derivative. On the contrary, VEoS proves to be efficient and renders elastic properties con-

sistently.

Also we contribute our theoretical assessments on EoS of the magnesium postperovskite, which is still covered much less in the literature, compared to the vast materials on the perovskite phase. Similarly, BMEoS of lower orders is found inappropriate. Controversially, VEoS may be insufficiently flexible to describe the postperovskite compression, possibly overestimating the bulk modulus.

# 2 Model

Quantum-mechanical calculations were performed with the CRYSTAL09 software package (Ref. [4, 5]), which implements the Hartree-Fock and Kohn-Sham Self Consistent Field (SCF) methods (Ref. [26]). For the perovskite model we used a hybrid Density Functional Theory Hamiltonian WC1LYP that adopts 84% of the Wu-Cohen exchange term, recently suggested in Ref. [35], and 16% of the Hartree-Fock term, alongside the Lee-Yang-Parr correlation term (Ref. [15]). In the case of postperovskite we opted for a widely applied hybrid Hamiltonian B3LYP (e.g. see in Ref. [12]). Linear Combination of Atomic Orbitals (LCAO) was adopted as the basis set in the form of Gaussian-type functions, with the original parameters of Ref. [25] adjusted to our models according to the variational principle.

Initial crystal structures of magnesium perovskite ($pv$) and postperovsite ($ppv$) from Ref. [9, 22] were first optimized in the Born-Oppenheimer approximation (athermal limit) with respect to the static lattice energy. Then a series of optimization was conducted under unit cell volume constraints to sample the static lattice energy as a function of volume ($V$). As implemented in CRYSTAL09, the normal mode frequencies of atomic vibrations were computed from the derivatives of lattice energy evaluated numerically at the zero wave vector. The Helmholtz free energy ($A$) of insulating solid was computed within the quasi-harmonic approximation as the sum of static lattice energy and the thermal contribution of vibrational frequencies (Ref. [1]).

The calculated Helmholtz energy at the set of unit cell volumes and the temperature of interest was then fitted to a polynomial $\sum_{j=0}^{N} a_j V^j$, first, by the minimax method (MM) (Ref. [27]) and, then, by the least squares method (LSQ). We opted for the biggest possible degree of approximating polynomial that delivered the solution of optimization problem in the uniform norm. The LSQ optimization was performed to validate the reliability of results and to control the precision, because its solution should converge to that of MM (Ref. [34]). The approximating polynomial was used to compute the pressure $P = -\frac{\partial A}{\partial V}$ and, subsequently, to apply the diagnostics of BMEoS and VEoS. The orders of polynomials were 6 for $pv$ (over 25 points of fitting) and 5 for $ppv$ (over 9 points of fitting).

A probe into the effect of phonon dispersion was made only on a subset of computed data for the pv series of calculations by employing a 2x2x2 supercell. The corrections to the calculated properties were beyond the presented precision.

Thus the phonon dispersion was ignored in the following materials.

# 3 Results and discussions

BMEoS originates from the Eulerian finite strain theory and is a model of common choice in the physics of minerals. Conventionally the strain is expressed as $f = \left[(V_0/V)^{2/3} - 1\right]/2$, where $V_0$ is the volume at zero pressure. Then BMEoS emerges in various orders from the Taylor expansion of Helmholtz Energy in terms of the strain around the minimum at zero pressure upon truncation of the series (Ref. [31]). There's a technique, commonly called the F-f plot, that is designed for a proper choice of the approximation level (Ref. [2]). It comprises a graphical representation of the normalized pressure $F = \frac{P}{3f(1+2f)^{5/2}}$ on the ordinate axis versus the strain $f$ on the abscissa. On the F-f plot BMEoS of the second (BM2), third (BM3) and forth order (BM4) correspond to a curve family graphs of a constant (horizontal line), a line and a parabola (quadratic polynomial), respectively.

In Fig. 1 we compare the $pv$ F-f plots of our model alongside the experimental data of Ref. [33, 7] at the room temperature. The theoretical dependence is clearly curved with a maximum at higher strains and varies approximately within an interval of 10 GPa. The points of measurements are scattered in a band of about 20 GPa or 10 GPa without the isolated outliers. The lower range of theoretical values should not surprise, as such deviation is due to the slight overestimation of the unit cell volume, common to quantum-mechanical models.

Legitimately, the authors of experimental works assumed a horizontal or subtly inclined linear trend, because the ponts sprawl in an irregular manner obscuring details of curvature. Failure of the assumption on such a large band, as the theoretical model predicts, leads to notable biases of inferred estimations of the elastic properties. For instance BM2EoS would overestimate the bulk modulus at zero pressure. BM3EoS optimized for data collected under high pressure would tend to undervalue the pressure derivative of bulk modulus, as approaching the extremum point it decreases significantly compared to the low strains value. Surely the experiments conducted mainly at high pressures would not fit with those operating at low strains, as Ref. [20] observed for the visualized measurements of Ref. [33, 7] for instance. Hence the higher order terms of BMEoS are critical for accurate estimations and the equations of lower orders than BM4 are inadequate to describe the isothermal compression on the inspected pressure intervals.

VEoS is an alternative compression model defined in terms of compression rate $x = (V/V_0)^{1/3}$ and is admissible when the plot of points $\ln H = \ln\left[\frac{Px^2}{3(1-x)}\right]$ vs. $(1-x)$ lie on a straight line (Ref. [2]). This diagnostics appears missing in the available literature, though the equation was applied to theoretical models of perovskite, as mentioned in the introduction. The respective plot is illustrated in Fig. 2 for the same data as of Fig. 1. It shows that the theoretical dependence indeed forms a straight line bellow the measurement points due to the

computational accuracy. Remarkably the experimental data are now arranged along the same line with the slope perfectly matching the theory. We conclude thus that VEoS is an appropriate model of compression for the perovskite.

Tbl. 1 suggests to compare numerically the estimations of elastic properties from various sources at the room temperature. As indicated in Ref. [28], the isothermal bulk moduli should be roughly about 5 GPa less than the adiabatic ones. Instead, BM2EoS renders their values greater up to 10 GPa, a bit less in experiments covering a narrower range of pressures. Except the theoretical calculation of Ref. [10], BM3EoS does not satisfy the thermodynamic relation either. On the contrary, VEoS returns the isothermal bulk moduli perfectly consistent with the adiabatic ones. This argument is very strong, as the adiabatic moduli in Tbl. 1 come from the direct measurements and should in principle excel the accuracy of the results inferred by fitting to an approximate EoS.

As anticipated in the introduction, the mineral is very stiff. Therefore a good quality of fitting requires to explore wide ranges of pressures maintaining a high precision of measurements. Unlikely, that the statistics of available data is sufficient to constrain as many parameters as in BM4EoS. Even with the lesser number of parameters, VEoS rather overestimates the pressure derivative of bulk modulus on the measurements of Ref. [33]. However the value is quite plausible once the data are extended by those of Ref. [7], while they still agree on the bulk modulus.

Considering the level of accuracy in the class of models, our numerical results are in a perfect agreement with the experimental estimations from VEoS. The results obtained by LSQ and MM are practically indistinguishable. It indicates that the solutions are convergent and well ensured within the precision of interest. The theoretical works of other authors, who adopted VEoS, do not match so well with the experiments though. Their procedure of parameters optimization is not discussed in details, but such large deviation could be caused by a sparse density of fitted points. Or one might surmise, they reduced the VEoS to a lower degree of approximation by fixing the pressure derivative value to that found in experiments through BMEoS. Such treatment permits to constrain the fitted parameters better. Nonetheless VEoS is quite sensitive to $K_0'$ and the error of 0.2-0.4 in the derivative might cause the observed discrepancy.

Fig. 3 presents the diagnostic plots for our models of *pv* and *ppv* together at the room and high temperatures. The F-f plots remain strongly curved and evidence the importance of 4th order term in BMEoS. Hence the interpretation of diagnostics for BMEoS pertains to the high temperature case, as well as to the postperovskite phase. The compression behavior of *pv* at the high temperature matches the model of VEoS, while the *ppv* phase reveals some curvature at the low strains. The curvature could be due to the low density of points around the 0 pressure: there's just one point at the negative strain and, indeed,the results of LSQ and MM optimization were subtly divergent in that region, which is important for the estimation of $V_0$ and hence the compression rate. Still, VEoS may overestimate the bulk modulus and underestimate the pressure derivative at 0 strain, so long as the curvature is not a numerical artifact. Therefore the postperovskite would possibly require a more flexible model of compression for

the accurate estimations.

The postperovskite is unstable at ambient conditions, therefore the measurements are conducted at elevated temperatures and pressures. Then they are extrapolated to infer the 0 pressure and room temperature properties. Consequently, such estimations suffer large inaccuracies. BM3EoS seems to overestimate the bulk modulus by around 15-25 GPa (Ref. [24, 8, 13]) with respect to ours (206 GPa) at ambient conditions. The theoretical works that adopt VEoS (Ref. [32, 22]) deliver results in the same range as experiments. Judging from our diagnostic plots, we believe, their values are possibly overestimated, though the hybrid Hamiltonian we used is known to underestimate the bulk modulus.

# 4 Conclusion

Our theoretical calculations demonstrated, that BMEoS up to the 3rd order fails to describe the compression of magnesium perovskite and postperovskite on the pressure ranges of geophysical interest. The discrepancy observed in Ref. [20] between the measurements conducted at high pressures, e.g. Ref. [7], and at low pressures (Ref. [33] and others), are most likely due to the chosen EoS. It appears to cause the systematic overestimation of the isothermal bulk modulus and the underestimation of its pressure derivative, as verified by the direct measurements of adiabatic bulk modulus. On the other hand, BM4EoS seems unpractical for experimental works, because the present statistics seems insufficient to constrain so many parameters of optimization.

However, our diagnostics reveals an excellent agreement between the Vinet model and the compression of perovskite. Indeed, the bulk moduli inferred from VEoS are perfectly consistent with the reported adiabatic bulk moduli. The experiments that are found to mismatch in the review of F-f plots by Ref. [20] demonstrate a perfect concordance in the diagnostic plot of Vinet model. Therewith the experiments are advised to adopt VEoS to improve the accuracy of their inference.

The isothermal compression of our postperovskite model deviates from VEoS in the vicinity of zero pressure. We expressed a doubt whether it's a computational artifact due to the low density of fitted points we set in that region. Is our diagnostic result true, the existed so far values of bulk moduli are perchance overestimated. The theoretical computations it is recommended to follow purely numerical methods like in this work, because they do not suffer the precision issues related to the measurements and they are robust against failures of the phenomenological models.

# References

[1] Anderson, O.L.: Equations of State of Solids for Geophysics and Ceramic Science. Oxford Monographs on Geology and Geophysics. Oxford University Press, New York, Oxford (1995)

[2] Angel, R.J.: Equations of state. Rev Mineral Geochem **41**, 35–60 (2000)

[3] Deng, L., Gong, Z., Fei, Y.: Direct shock wave loading of $MgSiO_3$ perovskite to lower mantle conditions and its equation of state. Phys Earth Planet In **170**(3-4), 210–214 (2008). DOI 10.1016/j.pepi.2008.07.043

[4] Dovesi, R., Orlando, R., Civalleri, B., Roetti, C., Saunders, V.R., Zicovich-Wilson, C.M.: CRYSTAL: a computational tool for the ab initio study of the electronic properties of crystals. Z Kristallogr **220**(5-6), 571–573 (2005)

[5] Dovesi, R., Saunders, V.R., Roetti, C., Orlando, R., Zicovich-Wilson, C.M., Pascale, F., Civalleri, B., Doll, K., Harrison, N.M., Bush, I.J., D'Arco, P., Llunell, M.: CRYSTAL09 Users Manual. University of Torino, Turin (2009)

[6] Fiquet, G., Andrault, D., Dewaelea, A., Charpinb, T., Kunz, M., Hausermannc, D.: P-V-T equation of state of $MgSiO_3$ perovskite. Phys Earth Planet In **105**(1-2), 21–31 (1998). DOI 10.1016/S0031-9201(97)00077-0

[7] Fiquet, G., Dewaele, A., Andrault, D., Kunz, M., Bihan, T.L.: Thermoelastic properties and crystal structure of $MgSiO_3$ perovskite at lower mantle pressure and temperature conditions. Geophys Res Lett **27**(1), 21–24 (2000). DOI 10.1029/1999GL008397

[8] Guignot, N., Andrault, D., Morard, G., Bolfan-Casanova, N., Mezouar, M.: Thermoelastic properties of post-perovskite phase $MgSiO_3$ determined experimentally at coremantle boundary PT conditions. Earth Planet Sc Lett **256** (2007)

[9] Horiuchi, H., Ito, E., Weidner, D.J.: Perovskite-type $MgSiO_3$; single-crystal x-ray diffraction study. Am Mineral **72**(3-4), 357–360 (1987)

[10] Karki, B.B., Wentzcovitch, R.M., de Gironcoli, S., Baroni, S.: Ab initio lattice dynamics of $MgSiO_3$ perovskite at high pressure. Phys Rev B **62**(22), 14,75014,756 (2000). DOI 10.1103/PhysRevB.62.14750

[11] Knittle, E., Jeanloz, R.: Synthesis and equation of state of (Mg,Fe) $SiO_3$ perovskite to over 100 gigapascals. Science **235**(4789), 668–670 (1987). DOI 10.1126/science.235.4789.668

[12] Koch, W., Holthausen, M.C.: A Chemists Guide to Density Functional Theory, 2nd edn. Wiley-VCH Verlag GmbH, Weinheim, New York, Chichester, Brisbane, Singapore, Toronto (2001)

[13] Komabayashi, T., Hirose, K., Sugimura, E., Sata, N., Ohishi, Y., Dubrovinsky, L.S.: Simultaneous volume measurements of post-perovskite and perovskite in $MgSiO_3$ and their thermal equations of state. Earth Planet Sc Lett **265** (2008)

[14] Kudoh, Y., Ito, E., Takeda, H.: Effect of pressure on the crystal structure of perovskite-type $MgSiO_3$. Phys Chem Miner **14**(4), 350–354 (1987). DOI 10.1007/BF00309809

[15] Lee, C., Yang, W., Parr, R.G.: Development of the Colle-Salvetti correlation-energy formula into a functional of the electron density. Phys Rev B **37**(2), 785789 (1988). DOI 10.1103/PhysRevB.37.785

[16] Li, B., Zhang, J.: Pressure and temperature dependence of elastic wave velocity of $MgSiO_3$ perovskite and the composition of the lower mantle. Phys Earth Planet In **151**(1-2), 143–154 (2005). DOI 10.1016/j.pepi.2005.02.004

[17] Mao, H.K., Hemley, R.J., Fei, Y., Shu, J.F., Chen, L.C., Jephcoat, A.P., Wu, Y., Bassett, W.A.: Effect of pressure, temperature, and composition on lattice parameters and density of $(Fe,Mg)SiO_3$-perovskites to 30 GPa. J Geophys Res **96**(B5), 8069–8079 (1991). DOI 10.1029/91JB00176

[18] Marton, F.C., Cohen, R.E.: Constraints on lower mantle composition from molecular dynamics simulations of $MgSiO_3$ perovskite. Phys Earth Planet In **134**(3-4), 239–252 (2002). DOI 10.1016/S0031-9201(02)00189-9

[19] Matsui, M.: Molecular dynamics simulation of $MgSiO_3$ perovskite and the 660-km seismic discontinuity. Phys Earth Planet In **121**(1-2), 77–84 (2000). DOI 10.1016/S0031-9201(00)00161-8

[20] Mosenfelder, J.L., Asimow, P.D., Frost, D.J., Rubie, D.C., Ahrens, T.J.: The $MgSiO_3$ system at high pressure: Thermodynamic properties of perovskite, postperovskite, and melt from global inversion of shock and static compression data. J Geophys Res **114**(B01203) (2009)

[21] Murakami, M., Hirose, K., Kawamura, K., Sata, N., Ohishi, Y.: Post-perovskite phase transition in $MgSiO_3$. Science **304**(5672), 855–858 (2004). DOI 10.1126/science.1095932

[22] Oganov, A.R., Ono, S.: Theoretical and experimental evidence for a post-perovskite phase of $MgSiO_3$ in earths d" layer. Nature **433**, 445–448 (2004). DOI 10.1038/nature02701

[23] Oganov, A.R., Price, G.D.: Ab initio thermodynamics of $MgSiO_3$ perovskite at high pressures and temperatures. J Chem Phys **122**(12, 124501) (2005). DOI 10.1063/1.1869973

[24] Ono, S., Kikegawa, T., Ohishi, Y.: Equation of state of $CaIrO_3$-type $MgSiO_3$ up to 144 gpa. Am Mineral **91**(2-3), 475–478 (2006). DOI 10.2138/am.2006.2118

[25] Ottonello, G., Civalleri, B., Ganguly, J., Zuccolini, M.V., Noel, Y.: Thermophysical properties of the $\alpha$-$\beta$-$\gamma$ polymorphs of $mg_2sio_4$: a computational study. Phys Chem Miner **36**(2), 87–106 (2009)

[26] Pisani, C., Dovesi, R., Roetti, C.: Hartree Fock Ab Initio Treatment of Crystalline Systems, 1st edn. Lecture Notes in Chemistry. Springer-Verlag, Berlin, Heidelberg, New York (1988)

[27] Powell, M.J.D.: Approximation theory and methods. Cambridge University Press, Cambridge, New York, Melbourne (1981)

[28] Ross, N.L., Hazen, R.M.: High-pressure crystal chemistry of $MgSiO_3$ perovskite. Phys Chem Miner **17**(3), 228–237 (1990). DOI 10.1007/BF00201454

[29] Saxena, S.K., Dubrovinsky, L.S., Tutti, F., Bihan, T.L.: Equation of state of $MgSiO_3$ with the perovskite structure based on experimental measurement. Am Mineral **84**(3), 226–232 (1999)

[30] Sinogeikin, S.V., Zhang, J., Bass, J.D.: Elasticity of single crystal and polycrystalline $MgSiO_3$ perovskite by brillouin spectroscopy. Geophys Res Lett **31**(L06620) (2004). DOI 10.1029/2004GL019559

[31] Stacey, F.D., Brennan, B.J., Irvine, R.D.: Finite strain theories and comparisons with seismological data. Surv Geophys **4**(3), 189–232 (1981)

[32] Tsuchiya, T., Tsuchiya, J., Umemoto, K., Wentzcovitch, R.M.: Phase transition in $MgSiO_3$ perovskite in the earths lower mantle. Earth Planet Sc Lett **224**(3-4), 241248 (2004)

[33] Vanpeteghem, C.B., Zhao, J., Angel, R.J., Ross, N.L., Bolfan-Casanova, N.: Crystal structure and equation of state of $MgSiO_3$ perovskite. Geophys Res Lett **33**(L03306) (2006). DOI 10.1029/2005GL024955

[34] Walsh, J.L.: Interpolation and approximation by rational functions in the complex plane. American Mathematical Society, Providence, Rhode Island (1935)

[35] Wu, Z., Cohen, R.E.: More accurate generalized gradient approximation for solids. Phys Rev B **73**(23, 235116) (2006)

[36] Yagi, T., Mao, H., Bell, P.M.: Structure and crystal chemistry of perovskite-type $MgSiO_3$. Phys Chem Miner **3**(2), 97–110 (1982). DOI 10.1007/BF00308114

[37] Yeganeh-Haeri, A., Weidner, D., ITO, E.: Elasticity of $MgSiO_3$ in the perovskite structure. Science **243**(4892), 787–789 (1989). DOI 10.1126/science.243.4892.787

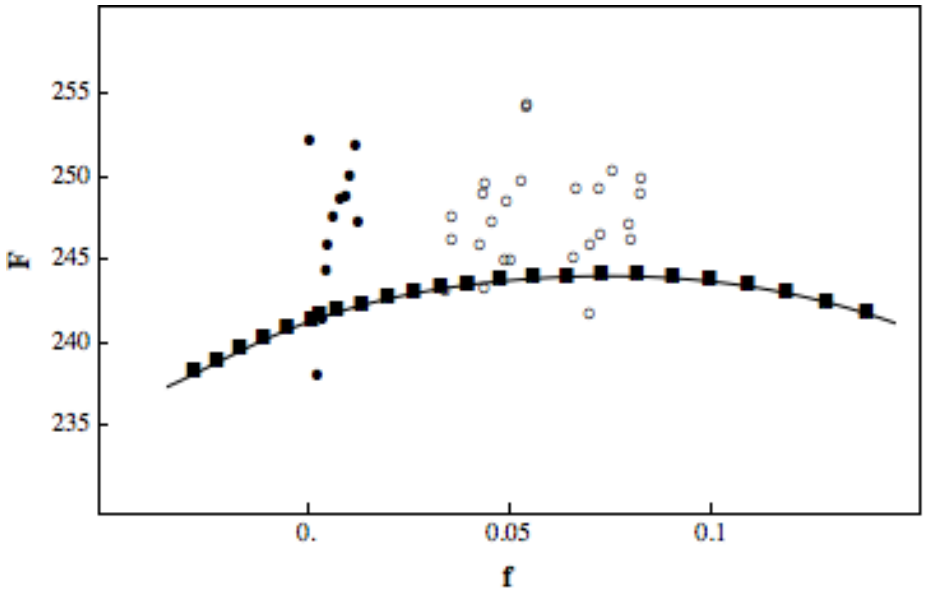


Figure 1: Room temperature F-f plot for perovskite: ■ and solid line - theoretical model; ○ - experimental data of Ref. [7]; • - experimental data of Ref. [33].

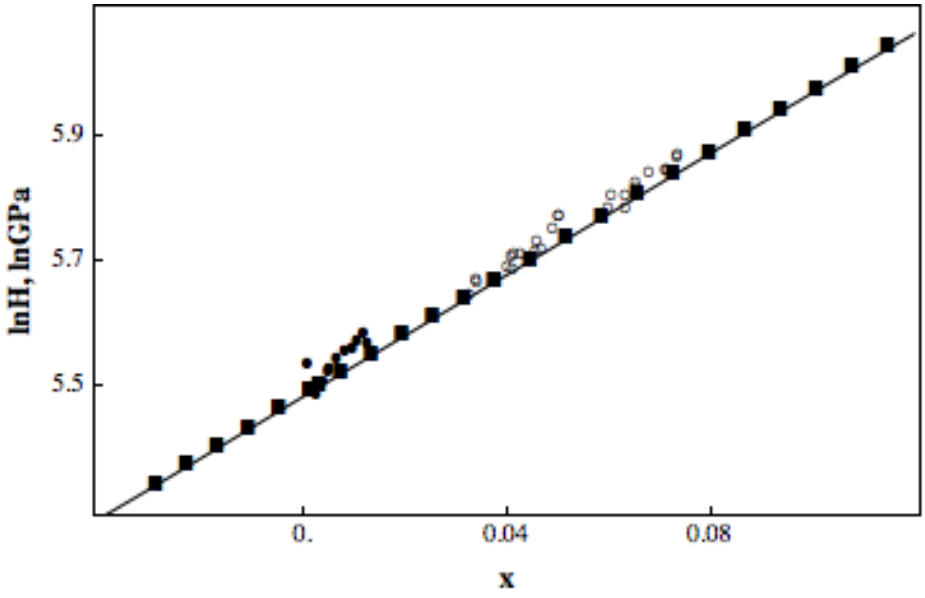


Figure 2: Room temperature diagnostic plot of VEoS for perovskite: ■ and solid line - theoretical model; ○ - experimental data of Ref. [7]; • - experimental data of Ref. [33].

Table 1: Isothermal and adiabatic bulk moduli: $K_0$ and $K_0'$ are the bulk modulus and its pressure derivative at 0 pressure; * denotes adiabatic properties; a) theoretical calculations; b) calculations performed in this work with the dataset of Ref. [33]; c) calculations performed in this work with the combined data of Ref. [33] and Ref. [7].

| Reference | $K_0$, GPa | $K_0'$ | $V_0$, Å$^3$ |
|---|---|---|---|
| BM EoS, 2nd order ($K_0'$ is fixed to 4) | | | |
| Ref. [28] | 254 | | 162.3 |
| Ref. [36] | 258 | | 162.8 |
| Ref. [14] | 247 | | 162.35 |
| Ref. [17] | 261 | | 162.5 |
| Ref. [6] | 256 | | 162.3 |
| Ref. [29] | 261 | | 162.4 |
| Ref. [33] | 253 | | 162.5 |
| BM EoS, 3rd order | | | |
| Ref. [11] | 266 | 3.9 | 162.8 |
| Ref. [7] | 253 | 3.9 | 162.3 |
| Ref. [10][a)] | 247 | 3.97 | 164.1 |
| Vinet EoS | | | |
| Ref. [23][a)] | 261 | 4.0 | 163.3 |
| Ref. [32][a)] | 248 | 3.9 | 164.1 |
| Ref. [19][a)] | 258 | 4.0 | 162.4 |
| Ref. [18][a)] | 273 | 3.9 | 162.5 |
| b) | 245 | 5.2 | 162.6 |
| c) | 244 | 4.2 | 162.6 |
| Other methods | | | |
| Ref. [37]* | 246.5 | | |
| Ref. [30]* | 253 | | |
| Ref. [16]* | 253 | 4.4 | |
| Ref. [3]* | 254 | 3.9 | |
| Ref. [20]* | 254-257 | 3.9-4.3 | |
| Polynomial approximation | | | |
| this work, pv, MM | 241 | 4.2 | 166.4 |
| this work, pv, LSQ | 241 | 4.2 | 166.4 |

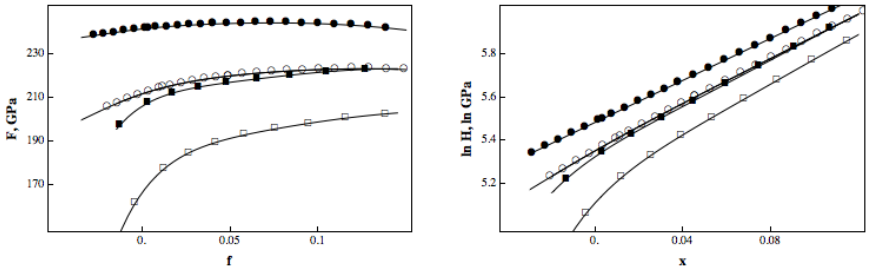


Figure 3: Diagnostic plots for BMEoS (left) and VEoS (right): ● - *pv* at 300 K; ○ - *pv* at 1000 K; ■ - *ppv* at 300 K; □ - *ppv* at 1000 K.